Thickness effect on nanoscale electromechanical activity in Pb(Mg1/3Nb2/3)O3-PbTiO3 thin films studied by piezoresponse force microscopy

A. Ferri, M. Detalle, J.F. Blach, M. Warenghem, Denis Remiens, R. Desfeux

Thickness effect on nanoscale electromechanical activity in $Pb(Mg_{1/3}Nb_{2/3})O_3$-$PbTiO_3$ thin films studied by piezoresponse force microscopy

Cite as: J. Appl. Phys. **110**, 104101 (2011); https://doi.org/10.1063/1.3660526
Submitted: 21 September 2011 • Accepted: 09 October 2011 • Published Online: 16 November 2011

A. Ferri, M. Detalle, J.-F. Blach, et al.

Thickness effect on nanoscale electromechanical activity in $Pb(Mg_{1/3}Nb_{2/3})O_3$-$PbTiO_3$ thin films studied by piezoresponse force microscopy

A. Ferri,[1,2,3,a)] M. Detalle,[4] J.-F. Blach,[1,2,3] M. Warenghem,[1,2,3] D. Rémiens,[5,6] and R. Desfeux[1,2,3]

[1]*Université Lille Nord de France, Lille F-59000, France*
[2]*Université d'Artois, Unité de Catalyse et de Chimie du Solide (UCCS), Faculté des Sciences Jean Perrin, Rue Jean Souvraz, SP18, Lens F-62307, France*
[3]*CNRS, UMR 8181, Villeneuve d'Ascq F-59650, France*
[4]*IMEC, Kapeldreef 75, Louvain B-3001, Belgium*
[5]*CNRS, UMR 8520, Villeneuve d'Ascq F-59655, France*
[6]*Institut d'Électronique de Microélectronique et de Nanotechnologie (IEMN), Département d'Opto-Acousto-Électronique (DOAE)/Matériaux et Intégration pour la Microélectronique et les Microsystèmes, Bâtiment P3, Cité Scientifique, Villeneuve d'Ascq F-59655, France*

(Received 21 September 2011; accepted 9 October 2011; published online 16 November 2011)

$0.7Pb(Mg_{1/3}Nb_{2/3})O_3$–$0.3PbTiO_3$ (PMN–PT) ferroelectric thin films with thickness ranging from 28 to 110 nm were sputter deposited onto $LaNiO_3/SiO_2/Si$ substrates. Optical properties were determined by spectroscopic ellipsometry. We found $B = 4.6$ and $\lambda_0 = 209$ nm, which is consistent for all PMN–PT samples with previous results shown in the literature. Nanoscale electromechanical activity was probed by using piezoresponse force microscopy in imaging and spectroscopic modes. Both piezoresponse images and local piezoloops recorded on each film highlighted an enhancement of piezoelectric vibration amplitude when the film thickness increased from 28 to 62 nm (~1.06 to ~1.34 mV), then saturation was observed for thicker films. This specific evolution was explained taking into account the low-permittivity interfacial $Pb_2Nb_2O_7$ layer existing between bottom electrode and PMN-PT layer. Higher leakage current when thickness is decreasing was shown, which could also explain the particular behavior of the local electromechanical properties. © *2011 American Institute of Physics*. [doi:10.1063/1.3660526]

I. INTRODUCTION

Ferroelectric thin films are attracting increasingly attention on account of the current development of highly minimized and integrated devices. In fact, their dielectric, piezoelectric, and ferroelectric properties were found to be promising for micro-/nanoelectronic technologies and micro-/nanomechanical applications.[1] However, progress in the elaboration of nanosystems, as well as the emergence of size effects caused by the miniaturization of devices, require the study and understanding of piezo-/ferroelectric properties of these films at the nanometer scale. In this respect, atomic force microscopy (AFM) in piezoresponse mode, i.e., piezoresponse force microscopy (PFM), has been developed as a powerful tool for imaging and control of submicron-scale domain structure in ferroelectrics.[2,3] It has thereby naturally emerged as the most appropriate technique for high-resolution electrical properties measurement of ferroelectric thin films. Among relaxor ferroelectric materials, $Pb(Mg_{1/3}Nb_{2/3})O_3$–$PbTiO_3$ (PMN–PT) compounds have received special attention because of their better dielectric and electrostrictive/piezoelectric properties.[4–7] The properties of such ferroelectric films strongly depend on many parameters, including preferred crystallographic orientation, composition, microstructure, thickness, existence of buffer layer, doping, domain configuration, etc.

In previous studies, we have investigated PMN–PT films deposited on conductive $LaNiO_3$ (LNO) electrodes with thickness ranging from 200 to 600 nm.[8,9] Nanoscale piezo-/ferroelectric properties were characterized by means of PFM technique. An interesting result was the similar local piezoelectric activity measured whatever the PMN–PT layer thickness. From this finding, we planned to synthesize thinner PMN–PT films in analogous experimental conditions to evaluate the piezoelectric vibration response when the ferroelectric layer thickness is reduced.

Therefore, in this paper, we report on PFM investigations focused on the role played by the film thickness, when reduced down to 28 nm, on the nanoelectromechanical properties of 0.7PMN–0.3PT ferroelectric films deposited onto $LaNiO_3/SiO_2/Si$ substrates.

II. EXPERIMENTAL

0.7PMN–0.3PT thin films were deposited by sputtering on SiO_2/Si substrates coated with conductive LNO bottom electrodes. As-deposited, PMN–PT films are amorphous and a conventional post-annealing performed at 450 °C is necessary to crystallize PMN–PT in perovskite phase. PMN–PT films with thicknesses ranging from 28 to 110 nm were

a)Author to whom correspondence should be addressed. Electronic mail: anthony.ferri@univ-artois.fr.

grown. Process parameters and details for growth could be found elsewhere.[8]

PMN–PT crystalline structure was investigated by x-ray diffraction (XRD) in the $\theta/2\theta$ scan mode using a Rigaku Miniflex+ diffractometer with filtered $CuK_{\alpha 1}$ radiation ($\lambda = 1.5406$ Å). The scan covered the 2θ range of 20–50° with steps of 0.01°.

The thickness and the optical properties of the ferroelectric layers were studied by spectroscopic ellipsometry (SE). SE measurements were performed at room temperature using a phase-modulated ellipsometer (UVISEL HR460 from Horiba Scientific) at wavelengths ranging from 400 to 800 nm with 1-nm intervals. An incidence angle of 70° was used for all measurements. The raw signal measured by SE has the following form: $I(t) = I(I_0 + I_S \sin(\delta(t)) + I_C \cos(\delta(t)))$, where $\delta(t)$ is a phase shift. In our experimental configuration, the value of I_0, I_C, and I_S are linked to the ellipsometric angles (Δ and Ψ) by the following relations: $I_0 = 1$, $I_S = \sin 2\Psi \sin \Delta$, and $I_C = \sin 2\Psi \cos \Delta$. The ellipsometric angles Δ and Ψ are related to the complex reflection coefficients of polarized light: R_p and R_s for a polarization parallel and perpendicular to the plane of incidence, respectively. For each sample, the measured spectra may be analyzed using an appropriate fitting model based on sample structure. All fitting steps were performed using the Delta-Psi 2 Horiba software.[10]

Surface morphology and associated roughness of the films were determined by AFM in contact mode. The piezoresponse mode of a modified commercial atomic force microscope (Multimode, Nanoscope IIIa, Digital Instruments) was used to get ferroelectric domain patterns. The spectroscopic tool of the PFM is used for measuring local amplitude piezoresponse loops.[2,3,8,11–13] In PFM imaging mode, an ac voltage is applied between the AFM conductive tip and grounded bottom electrode; whereas, for piezoloop measurements an ac signal superimposed on a dc bias voltage is applied between the tip and bottom electrode. Further experimental details about piezoloops recording can be found elsewhere.[14]

III. RESULTS AND DISCUSSIONS

XRD patterns for 28-, 53-, 62-, and 110-nm-thick PMN–PT films are given in Fig. 1(a). From the XRD experiments, all PMN–PT samples appear to be polycrystalline. (100), (110), and (111) peaks associated with the perovskite phase are observed in the 2θ range; no peak corresponding to the pyrochlore phase can be noted. A 4.05-Å out-of-plane lattice parameter is calculated, independently of film thickness.

Figure 1(b) presents typical AFM image of the PMN–PT films surface. The topographic image reveals a dense microstructure and a surface described by rounded grains with mean diameters slightly increasing with ferroelectric layer thickness, from 45 to 50 nm as reported in Table I. Values for similar PMN–PT films with thickness included between 200 and 600 nm and published in previous papers[8,9] are also indicated. Such an increase in grain size with thickness is commonly observed for grain structured ferroelectric thin films and could be associated with an uphill Ehrlich-Schwoebel-like growth mechanism, which tends to increase the growth of hills

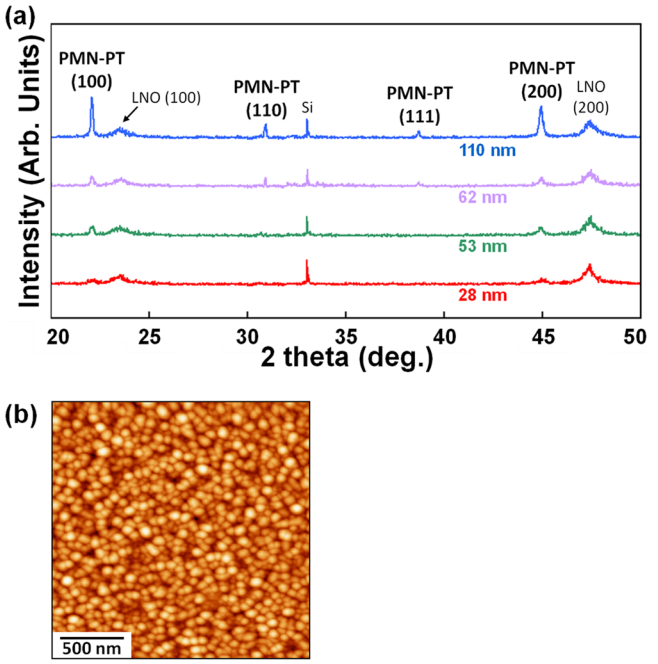

FIG. 1. (Color online) (a) X-ray $\theta/2\theta$ diffraction patterns of 0.7PMN–0.3PT films with thickness of 28, 53, 62, and 110 nm. (b) Typical AFM image of 0.7PMN–0.3PT thin films.

compared to valleys.[15,16] The root mean square roughness was measured over $5 \times 5\ \mu m^2$ surface area. A slight increase from 4.2 to 4.6 nm is observed when the thickness is ranging from 28 to 558 nm (see Table I).

To get information on the thickness of the synthesized PMN–PT layers, SE experiments were performed. From these measurements, optical properties have also been determined. From an optical point of view, PMN–PT films deposited on LNO bottom electrode were considered by a four-layers model (Fig. 2(a)): a silicon substrate covered by a passivation layer of SiO_2, the LNO electrode, and the PMN–PT film (we neglected the influence of the roughness layer). To obtain a reliable model, the first step consisted of finding the optical functions of each layer. The optical functions of Si and SiO_2 were found in the database of the Horiba Delta-Psi 2 software.[10] On the other hand, optical function of LNO layer was determined by fitting the ellipsometric spectra obtained by a sample of LNO layer deposited onto SiO_2/Si substrate. According to Hu *et al.*[17] and Mistrik *et al.*,[18] we can represent the optical function of LNO by a sum of a Drude function and double Lorentz oscillators as the following form:

TABLE I. Average lateral diameter of grains and root-mean-square roughness (R_{rms}) of the surface for 28-, 53-, 62-, 110-, 220-, 497-, and 558-nm-thick 0.7PMN–0.3PT films.

Thickness (nm)	28	53	62	110	220	497	558
Mean lateral diameter of grains (nm)	45	45	45	50	50	65	70
R_{rms} (nm)	4.2	4.2	4.2	4.3	4.3	4.4	4.6

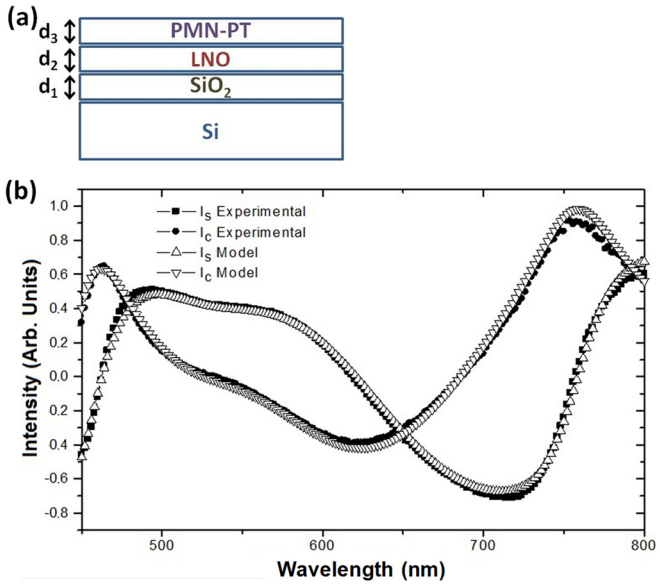

FIG. 2. (Color online) (a) Four-layers model of PMN–PT samples considered in spectroscopic ellipsometry measurements. (b) Example of ellipsometric spectra with the parameters I_s (from experiment and model) and I_c (from experiment and model) as a function of photon wavelength for a 70PMN–30PT thin film.

$$\varepsilon = \varepsilon_\infty + \frac{(\varepsilon_s - \varepsilon_\infty)\omega_t^2}{\omega_t^2 - \omega^2 + i\Gamma_0\omega} + \frac{\omega_p^2}{-\omega^2 + i\Gamma_D\omega} + \frac{f_1\omega_{01}^2}{\omega_{01}^2 - \omega^2 + i\gamma_1\omega}. \quad (1)$$

We obtained the following parameters for the optical function of LNO: $\varepsilon_\infty = 4.6$, $\varepsilon_s = 5.89$, $\omega_t = 2.67$ eV, $\omega_p = 4.29$ eV, $\Gamma_0 = 1.29$ eV, $\Gamma_D = 1.22$ eV, $f_1 = 1.75$, $\gamma_1 = 2.62$, and $\omega_{01} = 1.91$ eV. Where ε_∞ and ε_s are, respectively, the high-frequency and low-frequency dielectric constants; Γ_0, Γ_D, and γ_1 are the damping frequencies; ω_p represents the plasma frequency of the Drude model; ω_t and ω_{01} represent the resonant frequency of the two oscillators; and f_1 is the strength of the second oscillator. These parameters were then included in the four-layers model to gain access to the thicknesses and the optical function of PMN–PT film. DiDomenico and Wemple[19,20] have previously demonstrated that the optical function of oxygen-octahedral ferroelectrics can be modeled by a Sellmeier dispersion function without absorption. Moreover, the optical function of PMN–PT compound determined by SE in the visible spectral range was reported by various authors.[21–26] They also used a transparent Sellmeier function (Eq. (2)) as a model. In addition, we can mention the work of Chan *et al.*,[26] which demonstrated the extinction coefficient k of PMN–PT is fairly flat below 2.5 eV and thus can be neglected in the visible range. In this context, we adopted a transparent Sellmeier relation for our films by considering the fact we investigated the optical properties of ferroelectric layers in the visible optical range:

$$n^2 = 1 + \frac{S_0\lambda_0^2}{1 - \frac{\lambda_0^2}{\lambda^2}} = 1 + B\frac{\lambda^2}{\lambda^2 - \lambda_0^2}. \quad (2)$$

In this relation, λ_0 and S_0 represent the oscillator position and the average oscillator strength, respectively. The thicknesses of SiO_2, LNO, and PMN–PT layers and the optical function of PMN–PT film were obtained by fitting the ellipsometric spectra (Marquardt minimization algorithm). An example of result of the fit procedure is depicted in Fig. 2(b). The thicknesses of the films deduced from SE experiments are 28, 53, 62, and 110 nm. Each PMN–PT layer is thinner than previously studied films (i.e., 220, 497, and 558 nm for thick films in the range 200 to 600 nm as measured by SE), as expected for this work. The results (with notations in accordance with Fig. 2(a)) are summarized in Table II. Concerning the optical function of PMN—PT, we get a good agreement for all samples with the previous results shown in the literature. Indeed, we found $B = 4.6$ and $\lambda_0 = 209$ nm, whereas Tsang *et al.*[24] obtained $B = 4.66$ and $\lambda_0 = 216$ nm for 0.65PMN–0.35PT.

Nanoscale electrical properties measurements have been carried out by means of PFM. Ferroelectric domain pattern was observed by measuring the piezoresponse signal of the samples. Figure 3 depicts out-of-plane PFM images (OP–PFM), which were recorded on the surface of the PMN–PT films with 28, 53, 62, and 110 nm of thickness. Black, white, and intermediate contrasts are observed, whatever the film thickness. Such contrasts clearly demonstrate the presence of ferroelectric domains oriented normal and parallel to the film surface, and between these two perpendicular directions. This result is in a good agreement with the polycrystalline structure of the films. Indeed, domains with several directions for spontaneous polarization are expected when various oriented lattices exist in the ferroelectric layer.[8] In addition, such contrasted OP–PFM domains for all the films reflect the piezoelectric and ferroelectric state, whatever the thickness of the PMN–PT layer. As a result, PMN–PT films grown onto LNO bottom electrode are ferroelectric for thicknesses as small as 28 nm. However, it is interesting to note that the OP–PFM image corresponding to the thinner film (Fig. 3(a)) is less contrasted than those obtained for thicker films. Regions with intermediate contrasts are more important for 28-nm-thick PMN–PT film. This contrast difference may be explained by an upper density of domains where polarization vectors are deflected from film surface normal, or by a lower nanoscale piezoelectric activity. As the structure of thinner film is similar to one of thicker films (polycrystalline), the most reasonable explanation should be the lower vibration amplitude.

To confirm this assumption, measurements of local amplitude piezoresponse loops were carried out on each film. During loop recording, the AFM tip was located over the center of the small rounded grains observed at the film's surface, and whose PFM domain was the most contrasted on the corresponding

TABLE II. Results of ellipsometric measurements: d_1, d_2, and d_3 represent the thicknesses of SiO_2, LNO, and PMN–PT layers, respectively. The average error for the thicknesses determination is around 5 nm.

	Sample 1	Sample 2	Sample 3	Sample 4	Sample 5	Sample 6	Sample 7
d_1 (nm)	339	339	339	339	339	339	339
d_2 (nm)	45	45	45	48	45	45	45
d_3 (nm)	28	53	62	110	220	497	558

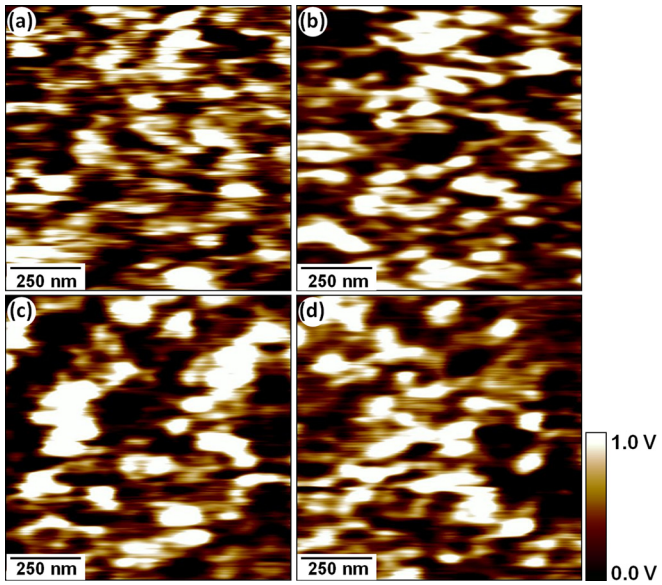

FIG. 3. (Color online) Out-of-plane PFM images recorded over the surface of (a) 28-, (b) 53-, (c) 62-, and (d) 110-nm-thick 0.7PMN–0.3PT films. The bar scale (0.0 V–1.0 V) is similar for the four images.

piezoresponse image (black region). Figure 4(a) shows a representative local amplitude piezoloop measured on the films. Specific dc voltages for domain switching under the tip were applied in respect to the film thickness. Indeed, for 62-, 53-, and 28-nm-thick films, dc voltages higher than ±5 V, more or less 5 V and ±3 V, respectively, could not be applied because

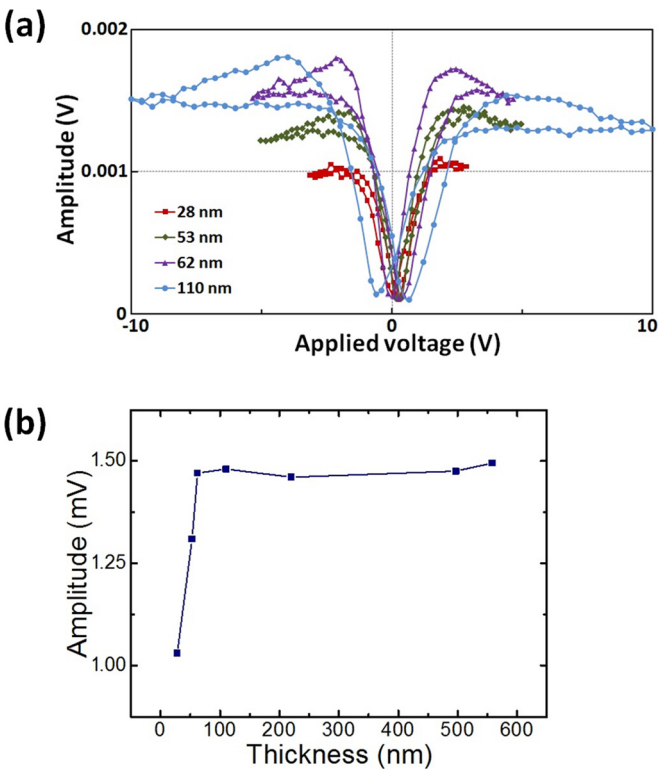

FIG. 4. (Color online) (a) Typical local amplitude piezoresponse loops recorded on 28-, 53-, 62-, and 110-nm-thick 0.7PMN–0.3PT films. (b) Evolution of local electromechanical activity of 0.7PMN–0.3PT thin films as a function of thickness.

of electrical breakdown effects that damaged the tip. Such effects are commonly obtained on films with such small thicknesses. For thicker films, dc voltage of ±10 V was applied. No significant effect of maximum dc voltage magnitude applied on the films was observed in local electromechanical activity measured on these PMN–PT films. Therefore, it is possible to compare the various piezoloops recorded on all the films, regardless of maximum and minimum dc signal value applied. The results show an enhancement in local piezoelectric vibration amplitude of PMN–PT layer when the thickness is increasing, until reaching saturation for a film thickness of 62 nm. Whereas the films having thicknesses from 62 nm present similar local average vibration amplitudes (~1.48 mV), the two thinner films (28 and 53 nm) are characterized by lower average piezoelectric activities (~1.06 and ~1.34 mV, respectively). Average values of vibration amplitude for 28-, 53-, 62-, and 110-nm-thick films studied in the present work and for thicker similar PMN–PT films already published[8,9] are reported in Table III. Evolution of these local electromechanical properties as a function of thickness of ferroelectric layer is plotted in Fig. 4(b). Increase of local piezoelectric response until film thickness is 62 nm, and then saturation above this characteristic thickness is clearly observed.

According to the literature, various behaviors were observed for local piezoelectric properties as a function of ferroelectric layer thickness. Nagarajan *et al.*[27] have shown for 0.9PMN–0.1PT films, that the piezoelectric coefficient d_{33} (pm/V) was multiplied by a factor ~8 for thicknesses varying from 100 to 400 nm. Hong *et al.*[28] have also shown that the vibration amplitude of the tip gradually increased from simple to approximately double with the $PbZrTiO_3$ (PZT) film thickness ranging from 40 to 152 nm. Meanwhile, Kim *et al.*[29] presented an increase of the longitudinal piezoelectric response d_{33} depending on the thickness of PZT films (thicknesses from 40 nm to 4 μm) deposited on $SrTiO_3$ substrates (d_{33} increasing from 20 to 330 pm/V) and on silicon (d_{33} enhancing from 10 to 200 pm/V). In contrast, Kim *et al.*[30] revealed an opposite evolution for piezoelectric coefficient d_{33} with the thickness of $PbTiO_3$ films: d_{33} is decreasing from the simple to triple when the film thickness is increasing from 60 to 200 nm. Finally, Nagarajan *et al.*[31] have shown that the d_{33} coefficient of PZT thin films was constant (60 pm/V) for a thickness larger than 20 nm, whereas the coefficient falls to 7 pm/V for 5-nm-thick films. These contrasted results reveal that no clear evolution is established for local electromechanical activity behavior as a function of ferroelectric film thickness.

To explain our results, we have considered the existing interfacial layer between LNO bottom electrode and PMN–PT film, as demonstrated in previous study.[32] This interfacial layer, identified as $Pb_2Nb_2O_7$, plays the role of buffer layer. Its thickness is about ~5 nm, as determined from HR–XRD

TABLE III. Average values for local piezoelectric vibration amplitude of 0.7PMN–0.3PT films with thickness ranging from 28 to 558 nm.

Thickness (nm)	28	53	62	110	220	497	558
Average amplitude (mV)	1.06	1.34	1.47	1.48	1.45	1.46	1.50

and transmission electron microscopy (TEM) measurements, whereas the permittivity is in the order of 65, as published elsewhere.[32,33] A relative permittivity value of around 1280 has been determined for PMN–PT films when the interfacial layer is not considered. Thus, the interfacial layer has to play a major role because of the small permittivity of this zone in comparison with the film. The thickness of the buffer layer is found to be constant whatever the thickness of the PMN–PT films. It is well known that the influence of the interfacial layer on the electrical properties of the films is directly related to the ratio between the ferroelectric layer and the interfacial layer thicknesses.[34,35] Hence, higher influence of the interfacial layer is expected for the thinnest films. This later consideration was established in a paper by Detalle *et al.*,[32] where relative permittivity of PMN–PT/$Pb_2Nb_2O_7$ heterostructure is decreasing with the PMN–PT layer thickness. In addition, it is established that the local piezoelectric properties are directly related to the permittivity of the ferroelectric film.[36] Indeed, the higher the dielectric permittivity, the larger the piezoelectric coefficient. As a consequence, an assumption to explain the smaller local electromechanical response measured in the case of thinnest films (28- and 53-nm-thick) would be the stronger influence of the low-permittivity interfacial $Pb_2Nb_2O_7$ layer. The fall of potential in this buffer layer would lead to a decrease of local piezoelectric response probed by the AFM tip.

In addition, we have not excluded the existence of a higher leakage current in thinner films for interpreting the specific local electromechanical behavior with film thickness. Indeed, effect of leakage current in thin films is more significant for small thicknesses. In our case, when PMN–PT thickness reaches values below 62 nm, the probing AFM tip could be more sensitive to the leakage-current effect in the ferroelectric layer, inducing the drop of local piezoelectric activity and thus the upper density of intermediate contrasts in OP–PFM image. This consideration is experimentally confirmed by both the need to apply specific lower dc voltage during the piezoloops acquisition in the case of thinner films, and by the impossibility to measure local current–voltage (I–V) curves by conductive-AFM because of the systematic electrical breakdown effects.

Consequently, the low-permittivity interfacial layer existing between bottom electrode and PMN–PT layer, associated with higher leakage current, could explain the electromechanical behavior of the PMN–PT films at such nanometer scale.

IV. CONCLUSION

In this paper, we have dealt with polycrystalline 0.7PMN–0.3PT films of 28-, 53-, 62-, and 110-nm-thickness deposited onto LNO/SiO_2/Si substrates. The optical properties determined by spectroscopic ellipsometry are consistent for all PMN–PT samples with the previous results shown in the literature. OP–PFM images demonstrated the coexistence of many types of ferroelectric domains, as expected in polycrystalline films. The PMN–PT films are ferroelectric for thickness as small as 28 nm. Local piezoelectric activity measured by piezoresponse loops was found to increase with the thickness for films from 28 to 62 nm, then saturation was observed until 558 nm. Such specific evolution was explained taking into account both the low-permittivity interfacial layer existing between bottom electrode and PMN–PT layer and the higher leakage current when thickness is decreasing. Further, the influence of a top electrode between the AFM tip and the ferroelectric film during measurements will be investigated in future work. Indeed, by considering that the electric field under such a top electrode is more homogeneous than under the AFM tip, fundamental in view of applications is to get information on the role played by a top electrode (with various lateral sizes) on "local" electromechanical activity as a function of the active layer thickness.

ACKNOWLEDGMENTS

The authors wish to acknowledge A. Da Costa for technical support and helpful discussions on AFM experiments, and L. Maës for technical support. This work was partially financially supported by the "Nord-Pas de Calais" region (France).

[1]J. F. Scott, Ferroelectrics **183**, 51 (1996).
[2]A. Gruverman, O. Auciello, and H. Tokumoto, Annu. Rev. Mater. Sci. **28**, 101 (1998).
[3]N. Balke, I. Bdikin, S. V. Kalinin, and A. L. Kholkin, J. Am. Ceram. Soc. **92**, 1629 (2009).
[4]S.-E. Park and T. R. Shrout, J. Appl. Phys. **82**, 1804 (1997).
[5]B. Noheda, D. E. Cox, G. Shirane, J. Gao, and Z.-G. Ye, Phys. Rev. B **66**, 054104 (2002).
[6]V. V. Shvarstsman and A. L. Kholkin, Phys. Rev. B **69**, 014102 (2004).
[7]K.-P. Chen, X.-W. Zhang, X.-Y. Zhao, and H.-S. Luo, Mater. Lett. **60**, 1634 (2006).
[8]A. Ferri, A. Da Costa, R. Desfeux, M. Detalle, G. S. Wang, and D. Rémiens, Integr. Ferroelectr. **91**, 80 (2007).
[9]A. Ferri, A. Da Costa, S. Saitzek, R. Desfeux, M. Detalle, G. S. Wang, and D. Rémiens, Ferroelectrics **362**, 21 (2008).
[10]HORIBA Jobin Yvon S.A.S., 5 Avenue Arago, Z. A. de la Vigne aux Loups, Chilly-Mazarin 91380, France.
[11]R. Desfeux, A. Ferri, C. Legrand, L. Maës, A. Da Costa, G. Poullain, R. Bouregba, C. Soyer, and D. Rémiens, Int. J. Nanotechnol. **5**, 827 (2008).
[12]S. V. Kalinin, A. N. Morozovska, L. Q. Chen, and B. J. Rodriguez, Rep. Prog. Phys. **73**, 056502 (2010).
[13]M. Detalle, A. Ferri, A. Da Costa, R. Desfeux, C. Soyer, and D. Rémiens, Thin Solid Films **518**, 4670 (2010).
[14]A. Ferri, S. Saitzek, A. Da Costa, R. Desfeux, G. Leclerc, R. Bouregba, and G. Poullain, Surf. Sci. **602**, 1987 (2008).
[15]R. Desfeux, A. Da Costa, and W. Prellier, Surf. Sci. **497**, 81 (2002).
[16]R. L. Schwoebel and E. J. Shipsey, J. Appl. Phys. **37**, 3628 (1966); G. Ehrlich and F. G. Hudda, J. Chem. Phys. **44**, 1039 (1966).
[17]Z. G. Hu, Z. M. Huang, Y. N. Wu, Q. Zhao, G. S. Wang, and J. H. Chu, J. Appl. Phys. **95**(8), 4036 (2004).
[18]J. Mistrik, T. Yamaguchi, D. Franta, I. Ohlidal, G. J. Hu, and N. Dai, Appl. Surf. Sci. **244**, 431 (2005).
[19]M. DiDomenico, Jr., and S. H. Wemple, J. Appl. Phys. **40**, 720 (1969).
[20]M. DiDomenico, Jr., and S. H. Wemple, J. Appl. Phys. **40**, 735 (1969).
[21]J. Q. Xue, Z. M. Huang, A. Y. Liu, Y. Hou, X. J. Meng, and J. H. Chu, J. Appl. Phys. **100**, 104107 (2006).
[22]A. Y. Liu, X. J. Meng, J. Q. Xue, J. L. Sun, J. Chen, and J. H. Chu, Appl. Phys. Lett. **87**, 072903 (2005).
[23]X. Wan, H. L. W. Chan, C. L. Choy, X. Zhao, and H. Luo, J. Appl. Phys. **96**(3), 1387 (2004).
[24]W. S. Tsang, K. Y. Chan, C. L. Mak, and K. H. Wong, Appl. Phys. Lett. **83**(8), 1599 (2003).
[25]K. Y. Chan, W. S. Tsang, C. L. Mak, and K. H. Wong, Phy. Rev. B **69**, 144111 (2004).
[26]K. Y. Chan, W. S. Tsang, C. L. Mak, and K. H. Wong, J. Eur. Ceram. Soc. **25**, 2313 (2005).
[27]V. Nagarajan, C. S. Ganpule, B. Nagaraj, S. Aggarwal, S. P. Alpay, A. L. Roytburd, E. D. Williams, and R. Ramesh, Appl. Phys. Lett. **75**, 4183 (1999).

[28]J. Hong, H. Wook Song, S. Hong, H. Shin, and K. No, J. Appl. Phys. **92**, 7434 (2002).
[29]D. M. Kim, C. B. Eom, V. Nagarajan, J. Ouyang, R. Ramesh, V. Vaithyanathan, and D. G. Schlom, Appl. Phys. Lett. **88**, 142904 (2006).
[30]Y. K. Kim, S. S. Kim, H. Shin, and S. Baik, Appl. Phys. Lett. **84**, 5085 (2004).
[31]V. Nagarajan, J. Junquera, J. Q. He, C. L. Jia, R. Waser, K. Lee, Y. K. Kim, S. Baik, T. Zhao, R. Ramesh, Ph. Ghosez, and K. M. Rabe, J. Appl. Phys. **100**, 51609 (2006).
[32]M. Detalle, G. Wang, D. Rémiens, P. Ruterana, P. Roussel, and B. Dkhil, J. Cryst. Growth **305**, 137 (2007).
[33]M. Detalle, D. Rémiens, G. Wang, P. Roussel, and B. Dkhil, Appl. Phys. Lett. **91**, 032903 (2007).
[34]L. Lian and N. R. Sottos, J. Appl. Phys. **87**, 3941 (2000).
[35]Z. Kighelman, D. Damjanovic, and N. Setter, J. Appl. Phys. **89**, 1393 (2001).
[36]R. Poyato, M. L. Calzada, V. V. Shvartsman, A. L. Kholkin, P. Vilarinho, and L. Pardo, Appl. Phys. A: Mater. Sci. Process. **81**, 1207 (2005).